Photochemistry

DOI: 10.1002/ange.201408816

Photochemically Induced Intramolecular Six-Electron Reductive Elimination and Oxidative Addition of Nitric Oxide by the Nitridoosmate(VIII) Anion

*Wyatt A. Thornley and Thomas E. Bitterwolf**

Abstract: *UV photolysis of the nitridoosmate(VIII) anion, OsO_3N^-, in low-temperature frozen matrices results in nitrogen–oxygen bond formation to give the Os^{II} nitrosyl complex $OsO_2(NO)^-$. Photolysis of the Os^{II} nitrosyl product with visible wavelengths results in reversion to the parent Os^{VIII} complex. Formally a six-electron reductive elimination and oxidative addition, respectively, this represents the first reported example of such an intramolecular transformation. DFT modelling of this reaction proceeds through a step-wise mechanism taking place through a side-on nitroxyl Os^{VI} intermediate, $OsO_2(\eta^2\text{-}NO)^-$.*

Oxidative addition and reductive elimination reactions are fundamental processes observed in transition metal chemistry. These are generally two-electron processes that are associated with addition or elimination of substrates such as H_2, alkanes, arenes, silanes, and others, and have been widely exploited in a variety of catalytic cycles. Far less common are the four- or six-electron analogues of these reactions.

Four- and six-electron oxidative addition of bonds in N_2O have been observed in a number of chemical systems.[1–3] In frozen gas matrices—metal atoms[4–9] and vacant metal sites generated through photochemical decarbonylation[10–13]—reactions have been observed with O_2, NO, and N_2 to form OMO, NMO, and NMN species, respectively. In some cases these products may be preceded by a η^2-XY species with conversion to the insertion product being either thermally or photochemically initiated. In an examination of the photochemistry of $CpW(CO)_2NO$ ($Cp = \eta^5\text{-}C_5H_5$) in frozen gas matrices, Rest and co-workers found evidence for intramolecular formation of an isocyanate ligand to give $CpW(CO)(NCO)$, presumably through the reaction of CO with a photochemically generated nitrene intermediate; the ultimate fate of the O-atom of the nitrosyl ligand remains elusive.[14] In a solution photolysis study of the closely related $CpMo(CO)_2NO$ in the presence of an excess of PPh_3, McPhail and co-workers found that in addition to the simple PPh_3 substitution product, generation of PPh_3O, $CpMo(CO)_2(NCO)PPh_3$, and $CpMo(CO)(NCO)(PPh_3)_2$ were also observed, providing evidence for intramolecular activation of the nitrosyl ligand to give an unobserved nitrene intermediate.[15] Finally, Legzdins and co-workers have observed isomerization of some 16-electron aryl and alkyl nitrosyl complexes of tungsten to the corresponding imido oxo analogues when in the presence of O_2 or H_2O; in the latter case an η^2-NO intermediate was suggested.[16–18]

Even less common are the four- and six-electron reductive elimination counterparts to these multielectron oxidative additions. We are only aware of two such examples that fit this category; the long-known photochemical ejection of O_2 from the permanganate ion[19–22] and S_2 from MS_4^{n-}, in which M, n = Mo, 2; W, 2; V, 3; and Re, 1 when in the presence of O_2.[23]

As part of our ongoing examination of metal nitrosyl photochemistry, our attention was directed toward the possibility that the photochemical nitrosyl bond cleavage reported by Rest and McPhail may occur through oxidative addition of a photogenerated η^2-NO intermediate. Oxidative addition of a η^2-NO may give rise to several valence isomers depending on the extent of reduction of the nitrosyl ligand, each possessing the same ligating atoms but differing in the nature of the bonds between the ligands and metal as well as the oxidation state of the metal. Formal four-electron oxidative addition of the nitrosyl ligand in $CpM(CO)_2(\eta^2\text{-}NO)$ would result in formation of what could be described as an anionic η^2-NO nitroxyl group and six-electron oxidative addition would result in cleavage of the NO bond to ultimately yield a mixed nitride oxide complex (Scheme 1).

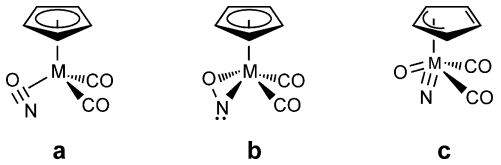

Scheme 1. Valence isomers of $CpM(CO)_2(\eta^2\text{-}NO)$.

Synthesis of four-electron valence isomers of a molybdenum nitroso complex has been previously reported. Wentworth and Maatta synthesized the η^2-nitrosobenzene complex $Mo(\eta^2\text{-}ONPh)(S_2CNEt_2)_2$ as well as its four-electron valence isomer $MoO(NPh)(S_2CNEt_2)_2$, a mixed phenylnitrene oxo complex.[24,25] Though no isomerization between $Mo(\eta^2\text{-}ONPh)(S_2CNEt_2)_2$ and $MoO(NPh)(S_2CNEt_2)_2$ was found to occur thermally nor following visible photolysis, in a subsequent publication we will demonstrate that this process does, indeed, occur at higher energies of incident light.[26] This remarkable example does demonstrate the ability of a transition metal to support such valence isomers as those proposed for the oxidative addition of an η^2-NO ligand.

[*] W. A. Thornley, Dr. T. E. Bitterwolf
Department of Chemistry, University of Idaho
875 Perimeter Dr, Moscow, ID 83844-2343 (USA)
E-mail: bitterte@uidaho.edu

Supporting information for this article is available on the WWW under http://dx.doi.org/10.1002/anie.201408816.

As no direct evidence for η^2-NO valence isomerism has been reported in metal nitrosyl photochemistry literature, we directed our focus on the photochemistry of model compounds that resemble the oxidative addition valence isomers of η^2-NO, that is, complexes with oxide and nitride ligands oriented in adjacent coordination sites. Microscopic reversibility indicates that if an η^2-NO ligand is capable of undergoing oxidative addition, that this family of compounds should then be able to reductively eliminate nitric oxide (Scheme 2). The MO_3N^{n-} family of compounds in which M, n = Mo, 3; Re, 2; and Os, 1 is matching this criteria.[27–29] Due to poor solubility of the polyanions, only $[(nC_4H_9)_4N)][OsO_3N]$ was found to be compatible with the matrix materials we currently use for low-temperature photolysis experiments.

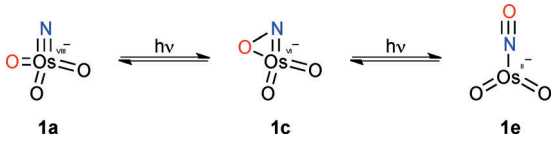

Scheme 2. Proposed reductive elimination of nitric oxide by OsO_3N^-.

The electronic spectrum of $[(nC_4H_9)_4N)][OsO_3N]$ as a thin film at 85 K in the region of 250–500 nm consists of three overlapping absorptions centered at 402, 357, and 315 nm with well-resolved vibronic fine structure (Figure 1). Mis-

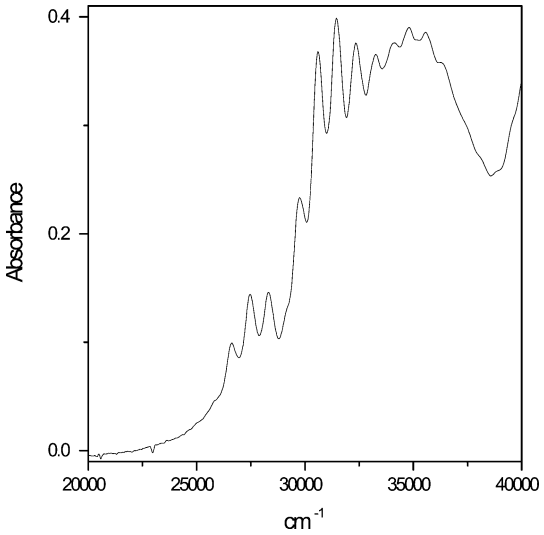

Figure 1. Electronic spectrum of $[(nC_4H_9)_4N)][OsO_3N]$ as a thin film at 85 K.

kowski and co-workers have previously performed a detailed analysis of the vibronic fine structure of the electronic spectrum of nitridoosmate(VIII) at 5 K, and found an average $\Delta\nu$ of 825 cm^{-1}, 900 cm^{-1}, and 872 cm^{-1} for the three absorptions bands, respectively.[30] This coupling corresponds to an 11–19 % reduction of the Os–N stretching frequency in the excited state, consistent with a ligand-to-metal charge transfer (LMCT) from the nitride ligand. TD-DFT calculations show that these three absorptions consist of vertical excitations from nonbonding nitride and oxide p-orbitals to molecular orbitals that are predominantly metal d-orbital in character. It is worth noting that the nonbonding nitrogen and oxygen p-orbitals of the LUMO are oriented in such a way that occupation of this orbital, accompanied by a molecular vibration along the C_s symmetry plane, may lead to a bonding N–O interaction (Figure 2).

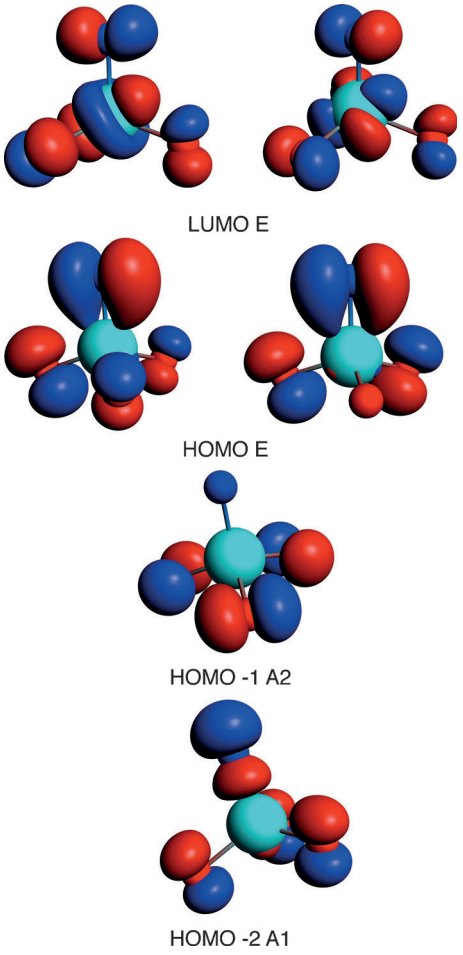

Figure 2. Selected Kohn–Sham orbitals of OsO_3N^- from nonrelativistic QZ4P/B88P86 calculation.

In a triethyloctylammonium tetrafluoroborate matrix at 85 K, $[(nC_4H_9)_4N)][OsO_3N]$ exhibits three well-resolved vibrational modes, an antisymmetric Os–O stretching mode at 872 cm^{-1}, a fully symmetric Os–O stretching mode at 889 cm^{-1}, and the Os–N stretch at 1014 cm^{-1} (982 cm^{-1} for the ^{15}N isotopomer; Figure 3). Photolysis of the sample at 330 ± 50 nm irradiation results in the bleaching of the parent vibrational bands, the growth of two new strong Os–O vibrational modes at 880 cm^{-1} and 918 cm^{-1}, and an intense absorption at 1620 cm^{-1} that shifts to 1584 cm^{-1} upon ^{15}N substitution (Figure 3a). Back photolysis of the 330 ± 50 nm irradiated sample with 400 ± 35 nm light results in reversion of the initial photoproduct to the parent compound (Figure 3b).

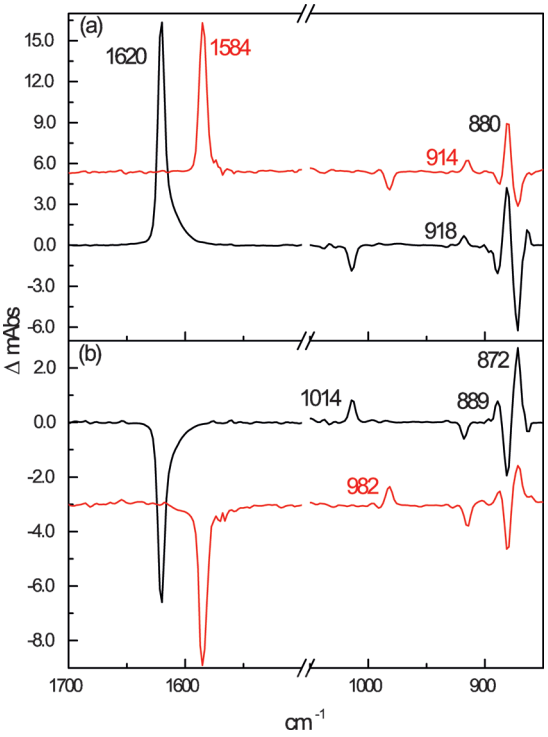

Figure 3. Photolysis of $[(nC_4H_9)_4N)][OsO_3N]$ in $[Oct_3EtN][BF_4]$ matrix at 85 K. a) Difference following 330 ± 50 nm irradiation from unphotolyzed sample. b) Difference following 400 ± 35 nm backphotolysis of 330 ± 50 nm irradiated sample. Results of photolysis of $[(nC_4H_9)_4N)][OsO_3{}^{15}N]$ presented as red trace.

The most notable feature of the 330 ± 50 nm irradiation photoproducts is the ^{15}N sensitive absorption at 1620 cm^{-1}. This new band lies within the metal–nitrosyl stretching region and well beyond the typical metal–oxo or metal–nitrido stretching region, demonstrating the generation of new N–O bonds in the molecule following UV photolysis. The weaker absorption at 918 cm^{-1} shifts to 914 cm^{-1} upon ^{15}N substitution, indicating that the molecular vibration is weakly coupled to the N atom. The ratio of the intensity of these two bands is highly dependent on the duration of photolysis, sample concentration, and the thickness of the matrix, suggesting that these vibrations belong to two different photoproducts. Back photolysis of these two products with 400 ± 35 nm light results in reversion to the parent complex at differing rates, demonstrating that the two photoproducts have overlapping electronic absorptions in this region.

Whereas the new absorption at 1620 cm^{-1} is strongly indicative of the presence of a linear metal–nitrosyl photoproduct, the identity of the secondary photoproduct primarily characterized by an absorption at 918 cm^{-1} is less clear. One possibility is the formation of a bond between two oxide ligands which would give rise to a peroxo O–O vibrational mode that would absorb in this region; however, the lack of any new absorptions assignable to the Os–N stretching mode of such a molecule makes this assignment unlikely. A more probable candidate is a species intermediate to the parent complex and the putative nitrosyl complex, that is, a species with a partially reduced metal center and a weak N–O bond

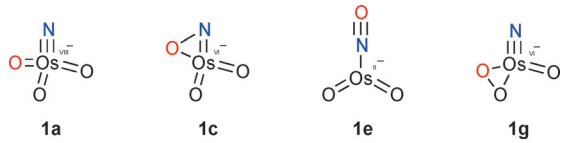

Scheme 3. Lowest-energy DFT stationary point geometries considered.

such as that of structure **1c** (Scheme 3). To clarify the nature of the photoproducts observed in our matrix photolysis experiments, a DFT investigation was performed to identify any possible species possessing N–O and O–O bonds.

DFT studies showed a single stationary point with a NO group in an η^2 coordination mode, a species possessing C_s symmetry analogous to **1c** calculated to lie 39.5 kcal mol^{-1} higher in energy than the parent complex. The elongated N–O bond length of 1.424 Å calculated for this species is consistent with a N–O bond. Previous DFT and photocrystallography experiments have demonstrated that nitrosyl N–O bond lengths remain nearly constant upon undergoing linkage isomerism,[31] suggesting that this elongation is not due to the mode of NO coordination, but rather the NO remaining highly anionic and better being described as an η^2-nitroxyl group. This would correspond to the metal having undergone a formal two-electron reduction. Calculated vibrational modes for this species, Table 1, show the expected

Table 1: Calculated QZ4P SO-TPSS-D3(BJ) vibrational frequencies (cm^{-1}) and intensities (km mol^{-1}) in parentheses for selected species. Values in red are those calculated for ^{15}N substitution.

Compound	Os–N	N–O	Os–O
OsO_3N^- (**1a**)	1039 (71.17) **1007 (60.20)**		892 (98.29) 881 (197.04) 875 (198.78)
$OsO_2(\eta^2\text{-NO})^-$ (**1c**)	696 (11.41) **684 (9.64)**	964 (40.79) **949 (7.44)**	923 (231.11) **919 (262.12)** 895 (241.60)
$OsO_2(\eta^1\text{-NO})^-$ (**1e**)	633 (38.69) **627 (36.07)**	1615 (592.74) **1577 (573.01)** O–O	892 (128.48) 873 (252.86)
$OsON(\eta^2\text{-}O_2)^-$ (**1g**)	1080 (82.80) **1047 (73.11)**	914 (58.66)	893 (212.24)

intensity of the N–O bond stretch to be much less than that of the Os–O stretching modes, offering an explanation as to why no ^{15}N sensitive N–O absorption is observed for this photoproduct. Compellingly, the fully symmetric Os–O stretching mode is weakly coupled to the N–O bond stretching mode and upon ^{15}N substitution is calculated to decrease in energy from 923 cm^{-1} to 919 cm^{-1}, consistent with the experimentally observed shift from 918 cm^{-1} to 914 cm^{-1}.

Only one stationary geometry was found that featured NO in an η^1 coordination mode, a C_{2v} symmetric complex with a linear nitrosyl group calculated to lie 27.6 kcal mol^{-1} higher in energy than the parent complex, **1e**. This geometry gave

calculated N–O and Os–O vibrational modes in excellent agreement with those observed in the matrix photolysis experiments. Formally, the Os metal center would be in the +2 oxidation state for this molecule, representing a net six-electron reduction from the parent complex. Additionally, a stationary geometry possessing a peroxo ligand, **1g**, was found to lie 61.2 kcal mol^{-1} higher in energy than the parent complex.

To better understand the relationship between these stationary points, transition state geometries on the potential energy surface were located; the results of these calculations are presented in Scheme 4. In all cases, calculated vibrational

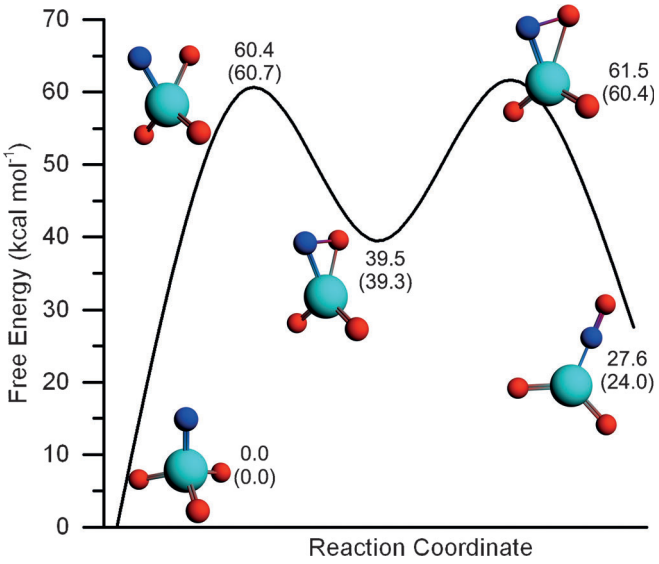

Scheme 4. SO-TPSS-D3(BJ) calculated reaction energy diagram for the observed photochemical transformation. Values in parentheses are from SR-B88P86 calculations.

modes of the transition states yielded a single large magnitude imaginary frequency and following the intrinsic reaction coordinate of these transition states yielded the expected stationary geometries. The barriers for the conversion of **1a** to **1c** and **1c** to **1e** are of very similar value at 60.4 kcal mol^{-1} and 61.5 kcal mol^{-1}, respectively. The barrier for the formation of **1g** was calculated at 86.4 kcal mol^{-1}, significantly higher in energy than that required for the formation of the nitrosyl species.

On basis of the results of DFT calculations, we dismiss the possibility of UV-photolysis-driven O–O bond formation to give an identifiable peroxo species in our low-temperature matrix photolysis experiments. The calculated barrier and stationary point energies for the peroxo complex are roughly 20 kcal mol^{-1} higher in energy than the corresponding N–O bond formation processes. Additionally, the absence of a new experimentally observable Os–N stretch in the photolysis products as well as the absence of any calculated ^{15}N coupled Os–O vibrational modes in the peroxo complex makes **1g** inconsistent as one of the observed photoproducts. We then identify the non-nitrosyl photoproduct generated during matrix photolysis as structure **1c**. DFT calculations found this partially reduced Os^{VI} species to connect the Os^{VIII} parent complex, **1a**, to the Os^{II} nitrosyl complex, **1e**, on the potential energy surface, making it a probable intermediate in the formation of the Os^{II} nitrosyl complex. Furthermore, the small magnitude shift of the symmetric Os–O vibrational mode upon ^{15}N substitution for complex **1c** is accurately reproduced by DFT. The identity of the species giving rise to the absorptions at 1620 cm^{-1} and 880 cm^{-1} is then assigned to complex **1e** which is fully consistent with experimental spectroscopic data and DFT calculations.

The exact mechanism of this transformation remains unclear. As the matrix photolysis experiments are conducted under steady-state photolytic conditions, multistep and multi-photon reactions are possible. In the present case, this would correspond to the absorption of a photon by the parent complex, **1a**, to form complex **1c**, which may then undergo secondary photolysis to form the nitrosyl complex **1e**. This would necessitate electronic overlap of **1a** and **1c** in the 330 ± 50 nm region to proceed in this manner. Furthermore, back photolysis of **1c** and **1e** with 400 ± 35 nm light results in reversion of both species to the parent complex, **1a**. Under these conditions, **1c** reverts to the parent complex faster than **1e** by comparison of the ratio of the two initially formed upon UV photolysis of the parent complex. This demonstrates electronic overlap of **1c** and **1e** assignable as metal-to-ligand charge transfer (MLCT) in this region with reversion of **1c** being the favored process. These data support a stepwise, two-photon process as opposed to a single-photon reaction that would be more likely to give only a single observable photoproduct.

In conclusion, a reversible photolytic six-electron reductive elimination and oxidative addition of nitric oxide by the nitridoosmate(VIII) anion has been demonstrated. To the best of our knowledge, this represents the first example of such a reaction. The results of this study offer a possible mechanism for the photochemical disproportionation of the nitrosyl ligand observed in previous studies. Moreover, this has broad implications for the development of catalytic small molecule activation that may be beneficial to the functionalization of abundant chemical feedstocks.

Experimental Section

$[(nC_4H_9)_4N)][OsO_3N]$ was prepared according to literature procedures.[30] $[(nC_4H_9)_4N)][OsO_3{}^{15}N]$ was prepared from 98% ^{15}N ammonium hydroxide supplied from Cambridge Isotope Laboratories. The apparatus and methods for matrix photochemistry have been reported elsewhere.[32]

All DFT calculations were performed in the Amsterdam Density Functional (ADF2013.01) program.[33–35] Electronic configurations of atoms were described by an all-electron quadruple-ζ Slater-type orbital basis set modified by four polarization functions (QZ4P STO).[36] Geometry optimizations and vibrational frequency calculations were performed using the GGA functional of Becke[37] and Perdew[38,39] as well as the dispersion corrected meta-GGA TPSS-D3(BJ).[40–42] Computations carried out using the B88P86 functional utilized a scalar relativistic correction, whereas TPSS-D3(BJ) computations used spin-orbit relativistic corrections within the Zeroth Order Regular Approximation (ZORA).[43,44] Open-shell calculations were performed to identify any possible S = 1 or S = 2 geometries, in all cases these were strongly energetically disfavored. The intrinsic

reaction coordinate (IRC) of all calculated transition state geometries was followed to confirm the relation with the expected stationary points. Electronic excitation energies were computed using SOC-B88P86 and the statistical average of orbital potentials (SAOP) model.[45,46]

Received: September 4, 2014
Published online: December 23, 2014

Keywords: nitrides · osmium · oxidative addition · photochemistry · reductive elimination

[1] W. B. Tolman, *Angew. Chem. Int. Ed.* **2010**, *49*, 1018 – 1024; *Angew. Chem.* **2010**, *122*, 1034 – 1041.
[2] J. P. F. Cherry, A. R. Johnson, L. M. Baraldo, Y. C. Tsai, C. C. Cummins, S. V. Kryatov, E. V. Rybak Akimova, K. B. Capps, C. D. Hoff, C. M. Haar, et al., *J. Am. Chem. Soc.* **2001**, *123*, 7271 – 7286.
[3] M. R. Lentz, J. S. Vilardo, M. A. Lockwood, P. E. Fanwick, I. P. Rothwell, *Organometallics* **2004**, *23*, 329 – 343.
[4] L. Andrews, M. Zhou, *J. Phys. Chem. A* **1999**, *103*, 4167 – 4173.
[5] A. Citra, L. Andrews, *J. Am. Chem. Soc.* **1999**, *121*, 11567 – 11568.
[6] M. Zhou, A. Citra, B. Liang, L. Andrews, *J. Phys. Chem. A* **2000**, *104*, 3457 – 3465.
[7] M. Zhou, L. Andrews, *J. Phys. Chem. A* **2000**, *104*, 3915 – 3925.
[8] X. Wang, M. Zhou, L. Andrews, *J. Phys. Chem. A* **2000**, *104*, 10104 – 10111.
[9] B. Liang, L. Andrews, *J. Phys. Chem. A* **2002**, *106*, 595 – 602.
[10] M. Poliakoff, K. P. Smith, J. J. Turner, A. J. Wilkinson, *J. Chem. Soc. Dalton Trans.* **1982**, 651.
[11] J. A. Crayston, M. J. Almond, A. J. Downs, M. Poliakoff, J. J. Turner, *Inorg. Chem.* **1984**, *23*, 3051 – 3056.
[12] M. J. Almond, J. A. Crayston, A. J. Downs, M. Poliakoff, J. J. Turner, *Inorg. Chem.* **1986**, *25*, 19 – 25.
[13] M. J. Almond, A. J. Downs, *J. Chem. Soc. Dalton Trans.* **1988**, 809.
[14] R. B. Hitam, A. J. Rest, M. Herberhold, W. Kremnitz, *J. Chem. Soc. Chem. Commun.* **1984**, 471.
[15] A. T. McPhail, G. R. Knox, C. G. Robertson, G. A. Sim, *J. Chem. Soc. A* **1971**, 205.
[16] P. Legzdins, M. A. Young, *Comments Inorg. Chem.* **1995**, *17*, 239 – 254.
[17] P. Legzdins, S. J. Rettig, K. J. Ross, R. J. Batchelor, F. W. B. Einstein, *Organometallics* **1995**, *14*, 5579 – 5587.
[18] P. Legzdins, S. J. Rettig, K. J. Ross, J. E. Veltheer, *J. Am. Chem. Soc.* **1991**, *113*, 4361 – 4363.
[19] M. Pougnet, *J. Pharm. Chim.* **1910**, *2*, 540.
[20] J. H. Mathews, L. H. Dewey, *J. Phys. Chem.* **1913**, *17*, 211 – 218.
[21] E. K. Rideal, R. G. W. Norrish, *Proc. R. Soc. London Ser. A* **1923**, *103*, 342 – 366.
[22] D. G. Lee, C. R. Moylan, T. Hayashi, J. I. Brauman, *J. Am. Chem. Soc.* **1987**, *109*, 3003 – 3010.
[23] A. Vogler, H. Kunkely, *Inorg. Chem.* **1988**, *27*, 504 – 507.
[24] E. A. Maatta, R. A. D. Wentworth, *Inorg. Chem.* **1979**, *18*, 2409 – 2413.
[25] E. A. Maatta, R. A. D. Wentworth, *Inorg. Chem.* **1980**, *19*, 2597 – 2599.
[26] W. A. Thornley, T. E. Bitterwolf, unpublished results.
[27] G. W. Watt, D. D. Davies, *J. Am. Chem. Soc.* **1948**, *70*, 2041 – 2043.
[28] A. F. Clifford, R. R. Olsen, S. G. Kokalis, T. Moeller, *Inorg. Synth.* **1960**, *6*, 167 – 169.
[29] J. Fritzsche, H. Struve, *J. Prakt. Chem.* **1847**, *41*, 97 – 113.
[30] V. Miskowski, H. B. Gray, C. K. Poon, C. J. Ballhausen, *Mol. Phys.* **1974**, *28*, 747 – 757.
[31] P. Coppens, I. Novozhilova, A. Kovalevsky, *Chem. Rev.* **2002**, *102*, 861 – 884.
[32] J. T. Bays, T. E. Bitterwolf, K. A. Lott, M. A. Ollino, A. J. Rest, L. M. Smith, *J. Organomet. Chem.* **1998**, *554*, 75 – 85.
[33] ADF2013, SCM, Theoretical Chemistry, Vrije Universiteit, Amsterdam, The Netherlands, http://www.scm.com.
[34] C. F. Guerra, J. G. Snijders, G. Te Velde, E. J. Baerends, *Theor. Chem. Acc.* **1998**, *99*, 391 – 403.
[35] G. Te Velde, F. M. Bickelhaupt, E. J. Baerends, C. Fonseca Guerra, S. J. A. van Gisbergen, J. G. Snijders, T. Ziegler, *J. Comput. Chem.* **2001**, *22*, 931 – 967.
[36] E. Van Lenthe, E. J. Baerends, *J. Comput. Chem.* **2003**, *24*, 1142 – 1156.
[37] A. D. Becke, *Phys. Rev. A* **1988**, *38*, 3098 – 3100.
[38] J. Perdew, *Phys. Rev. B* **1986**, *33*, 8822 – 8824.
[39] J. Perdew, *Phys. Rev. B* **1986**, *34*, 7406 – 7406.
[40] J. Tao, J. Perdew, V. Staroverov, G. Scuseria, *Phys. Rev. Lett.* **2003**, *91*, 146401.
[41] S. Grimme, J. Antony, S. Ehrlich, H. Krieg, *J. Chem. Phys.* **2010**, *132*, 154104.
[42] S. Grimme, S. Ehrlich, L. Goerigk, *J. Comput. Chem.* **2011**, *32*, 1456 – 1465.
[43] E. V. Lenthe, E. J. Baerends, J. G. Snijders, *J. Chem. Phys.* **1993**, *99*, 4597.
[44] E. van Lenthe, A. Ehlers, E. J. Baerends, *J. Chem. Phys.* **1999**, *110*, 8943.
[45] O. V. Gritsenko, P. Schipper, E. J. Baerends, *Chem. Phys. Lett.* **1999**, *302*, 199 – 207.
[46] P. R. T. Schipper, O. V. Gritsenko, S. J. A. van Gisbergen, E. J. Baerends, *J. Chem. Phys.* **2000**, *112*, 1344.